Author Manuscript

Author Manuscript

Author Manuscript

Author Manuscript

HHS Public Access

Author manuscript

J Neurochem. Author manuscript; available in PMC 2024 June 01.

Published in final edited form as:

J Neurochem. 2023 June ; 165(6): 827–841. doi:10.1111/jnc.15818.

Mice deficient for G-protein coupled receptor 75 display altered presynaptic structural protein expression and disrupted fear conditioning recall

Andrew Speidell[1,2], **Sofia Walton**[1], **Lee A Campbell**[1], **Francesco Tomassoni-Ardori**[3], **Lino Tessarollo**[3], **Claudia Corbo**[4,5], **Francesca Taraballi**[6,7], **Italo Mocchetti**[1,2]

[1]Laboratory of Preclinical Neurobiology, Department of Neuroscience, Washington, DC

[2]Interdisciplinary Program in Neuroscience, Georgetown University Medical Center, Washington, DC

[3]National Cancer Institute, Frederick, MD

[4]School of Medicine and Surgery Nanomedicine Center, University of Milano-Bicocca, Milan, Italy

[5]IRCCS Istituto Ortopedico Galeazzi, Milan, Italy

[6]Center for Musculoskeletal Regeneration, Houston Methodist Research Institute

[7]Orthopedics and Sports Medicine, Houston Methodist Hospital, Houston, TX

Abstract

There are a number of G-protein coupled receptors (GPCRs) that are considered “orphan receptors” because the information on their known ligands is incomplete. Yet, these receptors are important targets to characterize, as the discovery of their ligands may lead to potential new therapies. GPR75 was recently deorphanized because at least two ligands appear to bind to it, the chemokine CCL5 and the eicosanoid 20-Hydroxyeicosatetraenoic acid. Recent reports suggest that GPR75 may play a role in regulating insulin secretion and obesity. However, little is known about the function of this receptor in the brain. To study the function of GPR75, we have generated a knockout (KO) mouse model of this receptor and we evaluated the role that this receptor plays in the adult hippocampus by an array of histological, proteomic, and behavioral endpoints. Using RNAscope® technology we identified GPR75 puncta in several Rbfox3/NeuN positive cells in the hippocampus, suggesting that this receptor has a neuronal expression. Proteomic analysis of the hippocampus in 3-month-old GPR75 KO animals revealed that several markers of synapses, including synapsin 1 and 2 are downregulated when compared to wild type (WT). To examine the functional consequence of this down regulation, WT and GPR75 KO mice were tested on a

*Correspondence should be addressed to: Dr. Italo Mocchetti, Georgetown University Medical Center, Department of Neuroscience, WP13, New Research Building, 3970 Reservoir Rd, NW, Washington DC, 20057, Tel. 202-687-1197, fax 202-687-0617; moccheti@georgetown.edu.

Author’s contribution. AS designed, conducted and analyzed the behavioral experiments, and drafted a substantial portion of the manuscript; LC and SW completed the molecular biology and anatomical studies; FT-A and LT generated the KO animals; FT carried out the proteomic analyses; CC helped in the design of the proteomic analysis and performed the bioinformatic analysis; IM conceived and design the study, and drafted a substantial portion of the manuscript.

Conflict of interest. The authors declare no competing financial interests.

Author Manuscript Author Manuscript Author Manuscript Author Manuscript

hippocampal-dependent behavioral task. Both contextual memory and anxiety-like behaviors were significantly altered in GPR75 KO, suggesting that GPR75 plays a role in hippocampal activity.

Graphical abstract

GPR75 is a recently deorphanized G protein coupled receptor which is suspected to mediate unique properties of its cognate ligand, CCL5. In the present study, we examined the neural expression of GPR75 transcripts with a special emphasis on the hippocampus. We next employed CRISPR/Cas9 to generated a novel GPR75 knockout model and examined alterations in the hippocampal proteome in the absence of GPR75. Knockout mice were found to have down-regulation of major presynaptic neurotransmitter docking proteins vs wild type mice. We also report that knockout mice exhibit an impaired hippocampal-dependent recall of a trace interval.

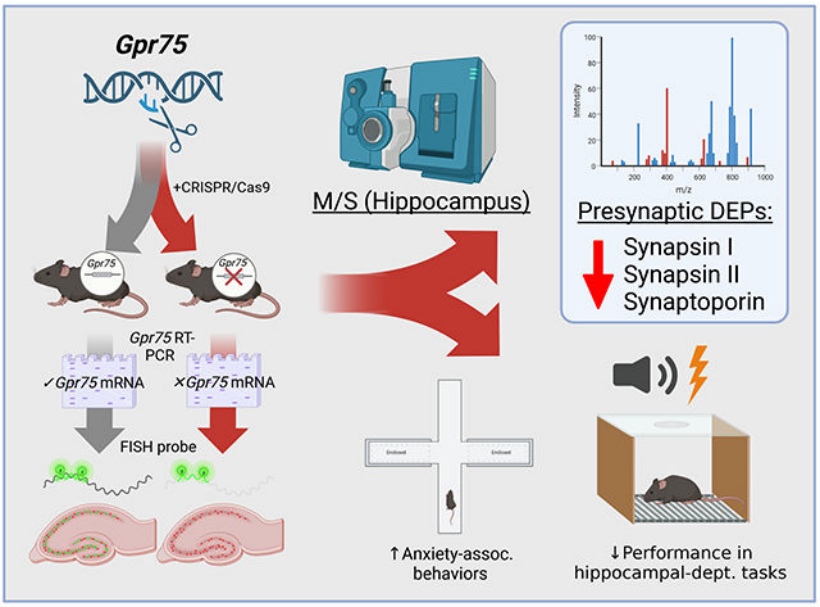

Keywords

CCL5; synapsin I and II; anxiety; GPR75; hippocampus

1. Introduction

G-protein coupled receptors (GPCRs) are a large class of evolutionarily-related cell membrane receptors. These receptors, when activated by ligands, initiate shared downstream signaling pathways through release of intracellular G protein subunits to modulate numerous cellular processes (Wootten et al. 2018). GPCRs have diverse physiological roles in virtually every organ system and possess a central role in the cellular response to extracellular endocrine and other molecular stimuli. Contribution of GPCR signaling is especially important for roles unique to the central nervous system (CNS), including developmental patterning (Kurabayashi et al. 2013, Luo et al. 2011), adult neurogenesis (Doze & Perez 2012, Matas-Rico et al. 2008), neuromodulation (Civelli 2012), and synaptic plasticity (Carr et al. 2003, Kempf et al. 2014, Sanderson et al. 2016). Moreover, there are a

Author Manuscript Author Manuscript Author Manuscript Author Manuscript

number of GPCRs that are considered “orphan” because they do not bind to any known neurotransmitters (Civelli et al. 2013). Yet, these receptors are important targets to discover new ligands and potential new therapies.

Originally listed in the orphan receptor family is the GPCR 75 (GPR75), a 540 amino acid member of the $G_{\alpha q}$ class of GPCRs, which contains seven transmembrane spanning domains, N-glycosylation sites in the N-terminus, and numerous serine and threonine phosphorylation sites in the C-terminus. (Tarttelin et al. 1999). Only recently, GPR75 has been shown to be activated by at least two ligands, the chemokine CCL5 (Dedoni et al. 2018, Ignatov et al. 2006) and the eicosanoid 20-Hydroxyeicosatetraenoic acid (20-HETE) (Garcia et al. 2017, Fan & Roman 2017). Activation of GPR75, like other $G_{\alpha q}$ family members, leads to induction of several signaling molecules including phospholipase Cγ (Liu et al. 2013), intracellular Ca^{2+} (Ignatov et al. 2006), inositol phosphate (Garcia et al. 2017), phosphatidylinositol 3–kinase (Ignatov et al. 2006) and its down-stream effector protein kinase B, also known as Akt.

Several existing reports indicate that GPR75 mRNA is expressed in the periphery (Liu et al. 2013) as well as in several brain areas (Sjostedt et al. 2020). In the periphery, this receptor appears to play a role in hypertension (Garcia et al. 2017), obesity (Akbari et al. 2021), glucose homeostasis (Powell et al. 2022, Liu et al. 2013) and prostate cancer (Cardenas et al. 2020). Less is known about the cellular localization and function of GPR75 in the brain. GPR75 has little homology to classical neurotransmitter (e.g., dopamine, serotonin) receptors (Tarttelin et al. 1999). In addition, GPR75 differs from known neural chemokine GPCRs in various key aspects. In contrast to the canonical CCL5 receptors (CCR5, CCR3, and CCR1), GPR75 has low expression in the spleen and other immune organs (Dedoni et al. 2018). Additionally, downstream cellular events elicited by GPR75 activation are mediated by release of the $G_{\alpha q}$ subunit of the G protein and not through $G_{\alpha i}$, which is uncharacteristic of other CCL5-responsive chemokine receptors (Dedoni et al. 2018, Ignatov et al. 2006).

Previous *in vitro* data have shown that GPR75 may possess a neuroprotective function in response to CCL5 (Dedoni et al. 2018, Ignatov et al. 2006). Moreover, many human limbic structures exhibit a relatively high gene expression of GPR75 (Sjostedt et al. 2020). Proper function of these critical anatomical subregions may therefore depend on the CCL5-GPR75 signaling during neural development or throughout adulthood. The extent to which neural GPR75 expression and signaling subserves morphogenic or functional roles remains wholly unexplored. In this study, we sought to explore the role of GPR75 within the CNS by generating and testing a knockout mouse model of this receptor. We then analyzed GPR75 mRNA expression in adult mice and carried out Tandem Mass Tag (TMT)-based proteomics analysis, and assessed behavioral endpoints in adult GPR75 KO mice and their wild type (WT) counterparts. We provide evidence that this receptor is abundant in the hippocampus and has an important role in hippocampal-dependent behavioral tasks.

Author Manuscript Author Manuscript Author Manuscript Author Manuscript

2. Materials and Methods

2.1 Generation of GPR75 knockout mice.

C57BL/6N mice obtained from a commercial source (Charles River Laboratories Inc., Frederick, MD), and maintained in the Division of Comparative Medicine's Research Resource Facility at Georgetown University Medical Center. All studies were carried out following the Guide for the Care and Use of Laboratory Animals as adopted and promulgated by the U.S. National Institutes of Health and approved by Georgetown University Animal Care and Use Committee (protocol number 2016-1188). Animals were allocated to each of the endpoints in our study arbitrarily. A flow-chart of the experimental procedures and animal groups is described in Fig. 1.

The GPR75 complete knockout mice (GPR75 KO) were generated by targeting the murine *GPR75* locus using the CRISPR/Cas9 DNA editing technology. Two specific sgRNAs were designed in the proximity of the GPR75 start-codon region (ATG) and two specific sgRNAs were designed in the proximity of the GPR75 stop-codon (TAA). A set of two sgRNAs (one sgRNA targeting the proximity of the start-codon and one sgRNA targeting the proximity of the stop-codon) were used in tandem without any DNA donor-template to generate a deletion of the *GPR75* coding region through non-homologous end joining DNA repair.

5' Guide RNAs (close to GPR75 start codon): #1 (Reverse): 5'-ATGTTTAGCAAGGTGGCATT-3' (PAM=GGG)

#2 (Forward): 5'-AACATGCCTCCCCTGCACGG-3' (PAM=GGG)

3' Guide RNAs (close to GPR75 stop codon): #1 (Forward): 5'-CACCACCAATGATTTGATGC-3' (PAM=AGG)

#2 (Reverse): 5'-TCAAGTGTTCAGTTGAGTCC-3' (PAM=AGG)

sgRNAs were generated *in vitro* using MEGAshortscript T7 transcription kit (cat.no. AM1354, Thermo Fisher Scientific, Waltham MA). Guide RNAs were then purified using MEGAclear kit (cat No AM1908, Thermo Fisher Scientific). Cas9 mRNA, 100 ng/μl (cat No L-7606, TriLink Biotechnologies, San Diego, CA), sgRNA5'#1 and sgRNA3'#1 or sgRNA5'#2 and sgRNA3'#2 (50 ng/μl) were microinjected (pronuclear microinjection) into one-cell stage zygotes obtained from C57BL/6Ncr × B6D2F1/J mice to generate GPR75-KO animals. Mice were screened by polymerase chain reaction (PCR) using the following primers: Forward: 5'-GTGTTTCCATTGCCTGGTTT-3'; Reverse: 5'-GTGGGGCTTCAATCAGGATA-3'. One founder mouse for each set of guide RNAs (set of sgRNA#1 and set of sgRNA#2) was chosen and further validated by DNA sequencing.

Founder mice were backcrossed to the C57BL/6N genetic background (Charles River Laboratories Inc., Frederick, MD) through interbreeding of at least 3 successive generations of GPR75 heterozygous (+/−) mice. After the backcrossing, $GPR75^{+/-}$ mice were intercrossed to obtain the wild type (WT) (used as controls), $GPR75^{+/-}$, and GPR75 KO mice used for all experiments. Once the KO was obtained, a total of 59 mice were used for the experiments. Genotype derived from each founder was verified by DNA sequencing.

Author Manuscript Author Manuscript Author Manuscript Author Manuscript

Animals were housed with their littermates approximately 2-5 mice per cage and were kept on a 12 h light-dark cycle beginning at 06:00 and ending at 18:00. Purina rodent chow #5001 (Purina Animal Nutrition LLC., Summit, MO) and Hydropac purified water (Lab Products Inc., Rockville, MD) were available *ad libitum* throughout the entire study. Unless otherwise stated, both males and females were used. No randomization method was used to allocate the animals in the study. No blinding was performed. No animals were excluded. Experimental mice were euthanized in the morning by intraperitoneal injection of 80/10 mg/kg Ketamine (cat.no. 5700864, Henry Schein Inc., Melville, NY) and xylazine (cat.no. 59399-110-20, Akorn Pharmaceuticals, Lake Forest, IL) mixture followed by intracardial perfusion of ice-cold phosphate buffered saline (PBS).

2.2 Confirmation of GPR75 knock-down.

2.2.1 Genomic DNA.—DNA was obtained from neural tissue from WT, GPR75$^{+/-}$, and GPR75$^{-/-}$ using the NucleoSpin Protocol (cat No 740952.50, Machery-Nagel, Düren, Germany). The PCR mix (25 µl) included Taq 2x Master Mix (cat No. M0270, New England Biolabs, Ipswich, MA), 0.2 µM Forward Primer, 0.2 µM Reverse Primer, nuclease-free water and 1 µl normalized gDNA.

2.2.2 Reverse Transcriptase-Polymerase Chain Reaction.—mRNA was extracted using the RNeasy Plus Mini Kit (Qiagen, Valencia CA, cat No. 74134). Samples were quantified on a Nanodrop and normalized to 250 ng/µl. 500ng of RNA was used as starting material for reverse transcription. RT-PCR was performed using the SuperScript™ IV VILO™ Master Mix (cat No. 11766050 Thermo Fisher Scientific,) and prepared according to the manufacturer's protocol. The resulting cDNA was quantified on a Nanodrop. Primers were used to detect excision of the GPR75 coding sequence; Forward (5'-ATCGTGTTGTCAGTCCTGGTG-3') and reverse (5'-CTGTTTGCAGCAGAGAAAGCC-3'). The PCR reaction T ran 1 cycle at 96°C for 2 min then a following 36 cycles at 94°C 1 min, 59°C 1 min 30s, and 72°C for 1 min 30 s. These cycles were then followed by 1 cycle of 72°C for seven minutes. The PCR products were run on a 1% Ultrapure agarose gel (cat. no.16500-500, Invitrogen, Waltham, MA) in 1x Tris-acetate-ethylenediaminetetraacetic acid (TAE) buffer 12.5 µl of DNA gel stain (cat no. S33102, Invitrogen).

2.3 Fluorescent Multiplex Detection with RNAscope®

(Fig. 1).RNAscope® was performed with Fluorescent Detection Kit v2. (cat. no. 323110, Advanced Cell Diagnostics Inc., Newark, CA) according to the manufacturer's pretreatment and assay protocol for formalin-fixed paraffin-embedded tissue. In brief, mouse brains were fixed in 10% neutral-buffered formalin, embedded in paraffin, dehydrated, sectioned at 5µm, and stained in the Georgetown Histology and Tissue Shared Resource. Staining for GPR75 mRNA was performed in the amygdaloid complex (Bregma −1.46 mm), and dorsal hippocampal formation (−2.18 mm). RNAscope® mouse probes for GPR75 (cat no. 318281) and RNA binding protein, fox-3 (RbFox3/NeuN, cat no. 313311-C2) were purchased from Advanced Cell Diagnostics Inc. and validated with positive and negative control probes for 2 hr at 40°C. The amplification steps were performed according to manufacturer's directions. Detection was performed by Opal Dye 570 (cat no. FP1488001KT, Akoya

Author Manuscript Author Manuscript Author Manuscript Author Manuscript

Biosciences, Marlborough, MA) for GPR75 and Opal Dye 620 (cat no. FP1495001KT, Akoya Biosciences,) for RbFox3. Brain sections were rinsed with PBS three times and incubated for 5 min in PBS with DAPI solution (1:50,000, Sigma-Aldrich, St. Louis, MO) for counterstained nuclei. Images were acquired on a Leica SP8 confocal microscope (Leica Microsystems, Wetzlar, Germany) in z-stacks (40x/1.4 magnification, 1024x1024, 200ms scanning speed, 0.3 μm/section, 1.2 μm stack total). Puncta in the anatomical region of interest were quantified by a blinded observer using CellProfiler (Broad Institute, Cambridge, MA).

Following *in situ* hybridization, the sections were processed for immunohistochemistry. Briefly, following the blocking step with 5% bovine serum albumin (BSA) in PBS for 1 h at room temperature (RT), post-hybridized slides were incubated with an antibody against glial fibrillary acidic protein (GFAP, 1:500, EMD Millipore, Temecula, CA), ionized calcium binding adaptor molecule-1 (Iba-1, 1:500, Wako Chemical USA, Richmond, VA), neuronal nuclear antigen (NeuN, 1:100, EMD Millipore) in the presence of 5% BSA in PBS overnight at 4°C. Brain slices treated with NeuN antibody were incubated for 72 h at 4°C. Subsequent to three washes with PBS, the slides were incubated with corresponding Alexa Fluor® 488 secondary antibodies (1:2000; Molecular probes®, ThermoFisher Scientific, Grand Island, NY) for 2 h at RT. Images were acquired on a Leica SP8 confocal microscope.

2.4. Preparation of synaptosomes and Western blot analysis.

Synaptosomes were prepared from hippocampal tissue using Syn-PER Synaptic Protein Extraction Reagent (cat.no. 87793, Thermo Fisher Scientific) according to the manufacturer's instructions and as previously described (Speidell et al. 2019, Speidell et al. 2020). Protein content was determined by BCA Protein Assay Reagent Kit (cat.no. 23225, Thermo Fisher Scientific) according to the manufacturer's instructions. Proteins were separated in a NuPAGE 4-12% Bis-Tris Gel (cat.no. NP0335, Invitrogen) and transferred to a PVDF membrane (cat.no. 1620117, Bio-Rad Laboratories, Hercules, CA). Membranes were blocked with 5% milk in PBS and 0.1% Tween-20 and probed with antibodies against GPR75 (cat. no. ab130666 Abcam, Waltham, MA; cat.no NBP1-59406 Novus Biological, LLC, Centennial, CO; cat. no. SAB4500182 Sigma-Aldrich). PSD95 antibody (1:2000, cat.no. MA1-045, Invitrogen) was used to confirm synaptosomes. To validate proteomic data, whole hippocampal tissue was homogenized in RIPA buffer (cat.no. 20-188, MilliporeSigma, Burlington, MA) containing Halt protease-phosphatase inhibitors (cat.no. 78442, Thermo Fisher Scientific). Electrophoresis and transfer of proteins were carried out as above and membranes were probed with Synapsin I (Sigma-Aldrich, cat. co # S193, 1:1000) or Synapsin II (Cell Signaling Technologies Danvers, MA. cat. no. #D6S9C, 1:1000). Membranes were stripped with Restore™ Western Blot Stripping Buffer (cat. no. 21059, Thermo Fisher Scientific Inc.) for 10 min at RT room temperature and re-probed with anti-β-actin antibody (1:10000-15000, cat. no. A1978 Sigma-Aldrich) in blocking buffer to serve as a protein loading control.

2.5 Tandem Mass Tag (TMT) Proteomics.

2.5.1 Protein preparation and enzymatic hydrolysis.—The hippocampus from WT and GPR75 KO was homogenized in lysis buffer containing 1% protease inhibitors

Author Manuscript Author Manuscript Author Manuscript Author Manuscript

by ultrasonic cracking. Lysates were centrifuged at 12,000g for 10 min at 4°C and the supernatant transferred to a new tube. Protein concentration was determined by bicinchoninic acid assay. Before enzymatic hydrolysis, proteins were first incubated in 5 mM dithiothreitol at 56°C for 30 min. Then iodoacetamine was added to make a final concentration to 11 mM and incubated at RT for 15 min, followed by trypsin, added at 1:50 mass at 37°C overnight.

2.5.2 TMT.—Peptides resulting from trypsin enzymatically processed proteins were vacuum freeze-dried after desalination by Strata X C18 (Phenomenex, Torrence, CA), then dissolved in 0.5 M triethylammonium bicarbonate (TEAB) (Sigma-Aldrich) and labeled according to the operating instructions of the TMT kit (Thermo Fisher Scientific). The operation was as follows: the labeled reagent was thawed and dissolved in acetonitrile, mixed with peptides and incubated at room temperature for 2 h and then the labeled peptides desalted after mixing and vacuum freeze-dried. 1 μg of samples were taken to be analyzed on the mass spectrometry.

2.5.3 High-performance liquid chromatography (HPLC) fractionation and liquid chromatography with tandem mass spectrometry analysis.—Peptides were fractionated by high pH reverse HPLC with column of 300 Extend C18 (Agilent Technologies, Santa Clara, CA). Peptides were graded at a gradient of 8% to 32% acetonitrile at pH 9, and 60 components were separated in 60 min. Then, peptides were combined into 18 components, and then were subjected to vacuum freeze drying for subsequent operation. Peptides were separated by an EASY-nLC 1000 ultra-high performance liquid phase system (mobile phase A: an aqueous solution containing 0.1% formic acid; mobile phase B: acetonitrile solution containing 0.1% formic acid). They were ionized into an NSI ion source and analyzed by Orbitrap Fusion Lumos mass spectrometry. The parent ions and secondary peptide fragments were detected and analyzed using high resolution Orbitrap with ion source voltage 2.4 kV (primary mass spectrometry scan range was set at 350-1550 m/z, scan resolution was set at 60,000; The scanning range of secondary mass spectrometry was fixed starting at 100 m/z, and the resolution of secondary scanning was set at 30,000).

2.5.4 Proteomic analysis and quantitation.—For processing the proteomics data, raw files were converted to mzML using MSConvert (Chambers et al. 2012). We used MASIC (Monroe et al. 2008) to calculate precursor ion intensities (derived from the area under each elution curve), and to extract reporter ion intensities. Butterworth smoothing method was used with a sampling frequency of 0.25 and an SIC tolerance of 10 ppm. Reporter ion tolerance was set to 0.003 Da with reporter ion abundance correction enabled. Spectra were searched with MSFragger (v3.5), ran with mass calibration (Kong et al. 2017, White et al. 1988). Protein inference and quantitation was performed by gpGrouper (v1.0.040) using shared peptide iBAQ area distribution (Saltzman et al. 2018). Resulting protein values were median normalized and log transformed for downstream analyses. Batch correction between multiplexes by ComBat (Johnson et al. 2007) as implemented in the Surrogate Variable Analysis package (Leek et al. 2012), version 3.44.0.

Author Manuscript Author Manuscript Author Manuscript Author Manuscript

2.6 Bioinformatic analysis.

Python 3.8 (Python Software Foundation) along with third-party library Pandas was used for data analysis. Among the 8500 identified proteins, we have selected differentially expressed proteins of interest using 1.2- fold change (both increase or decrease) and p-value < 0.05. Subsequently, multiple bioinformatics tools were employed to analyze this protein dataset in search of pathways/network of interest. These include David software to generate Gene Ontology (GO) annotation and the Kyoto Encyclopedia of Genes and Genomes (KEGG) database for the enrichment analysis of pathways. These pathways are classified according to KEGG hierarchical classification method.

2.7 Behavioral measures.

Rodents in this study were aged to ~12 weeks before beginning behavioral testing. At this time, experimenters gently handled animals each day for two days prior to the initiation of testing. Rodents in their home cage were taken from their vivarium room to the testing room and allowed to habituate to the new environment for 1 h prior to testing on each day. All mice were tested between 14:00 and 22:00 in their light-dark cycle. We ordered our behavioral measures to minimize the effect of repeated handling and anxiety in our mice. These measures were carried out within a three-week span in the order listed below.

2.7.1 Elevated Plus Maze.—The elevated plus maze (cat.no. 7001-0336, San Diego Instruments Inc., San Diego, CA) is a white platform raised approximately 75 cm off the floor of the testing room and lit with moderate overhead lighting (~100 lux). A camera above the apparatus tracked behaviors in the maze through Anymaze (Stoelting Co., Wood Dale, IL) over the 10 min trial. We assessed three measures in this apparatus: total time spent in the open arms of the maze, total entries to these open arms, and total distance travelled throughout the trial. The raw duration (to the nearest 0.1s) spent in the open arm were converted to percentage of trial (i.e., % trial) for our analyses.

2.7.2 Trace Fear Conditioning.—Trace fear conditioning was performed over three consecutive days via the procedure outlined by Lugo and colleagues (Lugo et al. 2014). Mice were exposed to two different contexts in this procedure. Context A consisted of a Ugo Basile fear conditioning apparatus (cat.no. 46003, Ugo Basile SRL, Gemonio, Italy) within a sound attenuating chamber. Context B was an empty reagent bucket with roughly similar floor surface area. These two contexts had different wall and ceiling patterns, floor textures, odorants, and were cleaned with different alcohols on each day. The apparatuses were lit with soft indirect light (~20 lux) and the foot shock was calibrated to 0.1mA. The conditional stimulus (CS) in both contexts was a 50dB 3kHz pure (sinusoidal) tone. There was soft white noise played within each trial to mask outside noises and the behavior within each context was recorded from an overhead camera and analyzed via Anymaze. Briefly, trace fear conditioning was performed in the following manner: Day 1 (Context A): 180s baseline (no stimulus) and 5x (20s CS + 20s trace period + 1s shock) with 120s intertrial interval. Day 2 (Context B): 120s baseline and 3x (20s CS + 20s trace period) with 120s intertrial interval. Day 3 (Context A): 8min with no CS and no shock. We recorded freezing behavior throughout the entirety of each test, but restricted our analyses to the baseline, CS presentation, and trace periods of each trial on days 1 and 2. The entire trial was evaluated

Author Manuscript Author Manuscript Author Manuscript Author Manuscript

for freezing behavior on day 3. We used the Anymaze software-recommended definition of freezing: greater than or equal to 1000 consecutive milliseconds without detectable motion in the apparatus. In our analyses, raw freezing time (recorded to the nearest tenth of a second) was first converted to percentage of the selected interval spent freezing (i.e., "% freezing") before statistical measures.

2.8 Statistical Analysis.

The study was not preregistered. No sample calculation or power analysis was performed. As there are no previous studies with this animal model, the required group size for biochemical and behavioral analyses was estimated based on existing animal studies from our laboratory (Bachis et al. 2016, Speidell et al. 2019) and others (Lievens et al. 2002, Wiltgen et al. 2005) with similar endpoints. Wilk-Shapiro tests for normality were performed on data sets before proceeding with parametric measures. If assumptions of parametric statistics were encountered, we used the two-tailed Mann-Whitney test. No animals or data points were excluded following ROUT analysis for outliers (Q=1%). Behavioral data, expressed as the mean ± SEM, were analyzed using one-way analysis of variance (ANOVA) with Bonferroni's multiple comparison post hoc test using GraphPad Prism software v. 5.0 (Graphpad Software Inc., San Diego, CA). Immunoblot data were analyzed via student's two-tailed t-test. To assess differences between groups for proteomic data, we used the moderated t-test as implemented in the R package *limma (*Ritchie et al. 2015*).* A P-value less than 0.05 after correction for false-discovery rate was considered to be significant. Multiple-hypothesis testing correction was performed with the Benjamini–Hochberg procedure (Hochberg & Benjamini 1990). Our overall experimental alpha level for significance was also 0.05.

2.9 Graphical abstract.

The graphical abstract and portions of the main figures were created with Biorender (http://www.biorender.com).

3. Results

3.1 Generation of GPR75 knock-out.

In the *mus musculus* genome, *GPR75* exists as one copy at a single genetic locus on chromosome 2; therefore, *GPR75* appears amenable to targeted genetic disruption. We employed a CRISPR-Cas9 approach to disrupt this locus and create a novel *GPR75* knockout model (Fig. 2). Successful knock-out of *GPR75* and lack of off-target insertions were confirmed via standard PCR on DNA obtained from neural tissue from young adult mice (Fig. 2B). A further lack of *GPR75* transcripts in the knockout group was demonstrated using end-point reverse transcription PCR on mRNA isolated from this same tissue. Fig. 2C shows that the expected 234 base band is reduced in GPR75 heterozygous mice and missing in the KO group.

In an effort to compare basic characteristics of this model with the existing human and preclinical data, we assessed body weight of two separate cohorts of mice at 12 and 26 weeks of age given free access to standard (i.e., non-high-fat) rodent chow. We found

Author Manuscript Author Manuscript Author Manuscript Author Manuscript

that 26-week-old GPR75KO males (n=26), but not females (n=25) mice, were resistant to age-related gains in body mass (Supplementary Figure 1), confirming previous studies that the perturbations in GPR75 expression is associated with reduction in body fat in mice and a lower prevalence of obesity in humans (Akbari et al. 2021, Powell et al. 2022).

3.2 GPR75 gene expression is predominantly localized to neurons.

Several commercially-available antibodies against GPR75 exhibit non-specific binding to murine neural antigens as determined by Western blot analyses of hippocampal lysates from WT and KO mice (Supplementary Figure 2). Thus, we used *in situ* hybridization to map the expression of GPR75 mRNA in adult mice (n=3 each group). We first validated the specificity of the GPR75 probe for RNAscope® by comparing GPR75 mRNA signal in brain sections from WT and KO mice. In the hippocampus (Fig. 3A) of WT mice, the GPR75 probe produced a strong fluorescent signal, characterized by green dots, localized in DAPI positive nuclei which contained the mRNA of the neuronal marker RbFox3 (Figs. 3B and C), suggesting that in the hippocampus GPR75 expression is mainly neuronal. No hybridization for GPR75 mRNA was observed in GPR75 KO mice (Fig. 3A), supporting the specificity of the GPR75 mRNA probe used for RNAscope®. There was no difference in RbFox3 positive neurons between WT and GPR75KO (not shown), suggesting that the removal of this receptor does not alter the total number of neurons.

Analysis of the hippocampal formation revealed that GPR75 mRNA is particularly abundant in the CA regions (Fig. 3D). The green puncta that correspond to GPR75 mRNA were found outside and inside the nuclei (Figs. 3B and C) suggesting that some of this mRNA is readily available for translation. GPR75 mRNA was also abundant in the basolateral amygdala (Fig. 3D). However, few green puncta were also observed in sections throughout the corpus callosum (Fig. 3D), suggesting that some non-neuronal cells may also express GPR75 or that this receptor might be present in axons. Semi-quantitative of puncta revealed that the hippocampus contains at least two-fold the amount of GPR75 when compared to the corpus callosum (Fig. 3D).

Our preliminary analysis indicates that in the hippocampus GPR75 mRNA hippocampus is mostly expressed in neurons. To reveal whether other cell type express this receptor, we examined the hippocampus utilizing RNAscope® *in situ* hybridization combined with immunohistochemistry for specific glial cell markers. These include GFAP, an astrocytic marker, and Iba-1, a microglia/macrophage-specific marker. We found that GFAP (Fig. 4B), and Iba-1 (Fig. 4C) positive cells were GPR75 negative, whereas the majority of NeuN positive cells contained GPR75 mRNA (Fig. 4A). These results validate the notion that the GPR75 mRNA is mainly expressed in neurons.

3.3 GPR75 KO exhibit altered hippocampal proteome profile.

We used mass spectrometry-based quantitative proteomic strategy to analyze the hippocampus of WT and GPR75KO (n=4, each group) for changes in synaptic protein composition due to the removal of GPR75. In total, we identified 8980 proteins with a TMT labeling efficiency of greater than 99%. In these samples, 63 proteins were up-regulated and 38 proteins were down-regulated in GPR75 KO when compared to WT ($p<0.05$). Volcano

Author Manuscript Author Manuscript Author Manuscript Author Manuscript

plot (log_{10} (P value) vs log_2 (fold changes) was constructed to graphically display the quantitative data (Fig. 5). Differentially abundant proteins were subjected to GO analysis to investigate KEGG pathways and molecular function (Fig. 6). Proteins significantly changed in GPR75 KO mice were primarily related to synaptic proteins, including neurotransmitter transporters and transcription factors. For example, synapsin 1 and 2, and synaptoporin are down-regulated in KO mice (Table 1). Western blot analyses of hippocampal lysates from WT and GPR75 KO mice confirmed a significant decrease in synapsin II in KO mice (supplementary figure 3).

3.4 GPR75 KO mice exhibit increased anxiety-like behaviors and display altered performance on hippocampal-dependent behavioral tasks.

Due to the high expression of GPR75 in limbic areas and the effects of its knock out on major synaptic protein expression, we hypothesized that constitutive lack of GPR75 may have an effect on amygdala- or hippocampal-dependent behaviors. We first assessed anxiety-like behaviors in the elevated plus maze between the genotypes in this study. Within a single 10-minute exposure to the apparatus, GPR75 KO mice spent significantly less time in the open arms (Fig. 7A, two-tailed student's t-test, $t_{[22]}=4.722$, $p<0.001$; and had fewer entries to these arms (Fig. 7B, two-tailed Mann-Whitney, $U=20$, $p<0.01$) when compared to WT. The behavior was done with more males than females, due to the use of females for breeding, however, we did not observe a sex-effect (trial open arms, males alone $t_{[14]}=4.048$, $p<0.01$; entries to open arms, $U=8.5$, $p<0.01$ when comparted to WT). There was no difference in total exploration activity between the genotypes in the elevated plus maze (Fig. 7C, two-tailed student's t-test, $t_{[22]}=0.2247$, $p=0.8243$; males $t_{[14]}=0.0936$, $p=0.9268$). To explore potential behavioral impairments on tasks of hippocampal-dependent learning and memory, we subjected the rodents in this arm of the study to a 3-day trace fear conditioning paradigm. As for data shown in Fig. 7, also in these groups, values for females fall within the range of values for males. Despite an observed increase in anxiety-related behaviors in GPR75 KO mice, baseline freezing behavior upon the introduction of mice to unfamiliar contexts A or B was equivalent among the experimental groups (Fig. 8B, two-tailed Mann-Whitney U test, $U=34.50$, $p=0.1554$; males $U=19$, $p=0.0886$ and Fig. 8C, $U=65.50$, $p=0.4596$; males $U=32.50$, $p=0.7650$, respectively). Additionally, freezing during the trace periods in conditioning trials was not significantly altered in GPR75 KO vs. WT mice (Fig. 8B, two-tailed student's t-test, $t_{[24]}=0.6854$, $p=0.4996$; males $t_{[15]}=0.7553$, $p = 0.4618$), suggesting no difference in the magnitude of the CS-foot shock association among experimental groups. However, the percentage of the trace period spent freezing in WT mice on Day 2 (representing trace recall) was significantly greater than in GPR75 KO counterparts (Fig. 8C, two-tailed student's t-test, $t_{[24]}=2.874$, $p<0.01$; males $t_{[15]}=2.011$, $p=0.062$). Contextual memory, assessed on day 3, was likewise altered in GPR75 KO mice (Fig. 8D, two-tailed student's t-test, $t_{[24]}=2.452$, $p<0.05$; males $t_{[15]}=3.226$, $p<0.01$). Our behavioral results suggest that removal of GPR75 is associated with significant perturbations in re-activation of hippocampal memory traces.

Author Manuscript Author Manuscript Author Manuscript Author Manuscript

4. Discussion

Cell-specific expression of a given receptor often reveals its role in cell communication and metabolic pathways, yet the identification of the precise roles orphan receptors fulfill is complicated by incomplete knowledge of their cognate ligands and the receptor's spatiotemporal expression profile. GPR75 is no exception to these issues. Recent reports describe activation of GPR75 by 20-HETE, which seems to play a role in the general metabolism that promotes obesity (Akbari et al. 2021, Gilani et al. 2021, Powell et al. 2022, Liu et al. 2013). Less is known about the function of GPR75 in the mature brain. In this study, we provide preliminary evidence that this receptor is expressed in adult hippocampal neurons and plays a role in limbic-associated behaviors, likely through an indirect mechanism which involves synapsin I, II and other major synaptic proteins.

A previous study has shown high GPR75 immunoreactivity in neurons, particularly in the perirhinal cortex and granule cell of the rat hippocampus (Gonzalez-Fernandez et al. 2020). Poor specificity of the existing anti-GPR75 commercial antibodies continues to limit interpretations of these results (Supplementary Figure 2). However, our RNAscope/*in situ* hybridization data confirm that in the hippocampus GPR75 mRNA is expressed mainly by neurons. In fact, we found that the majority of NeuN positive cells contain GPR75 mRNA puncta, whereas GFAP and Iba-I positive cells were GPR75 mRNA negative. Future studies will reveal whether the neuronal expression of GPR75 mRNA is retained throughout the CNS.

The behavior and proteomic data support a role for GPR75 in hippocampal function because GPR75 KO mice, which has lower synaptic markers when compared to WT, exhibit an impairment in hippocampal-dependent tasks, including contextual memory. Of course, we cannot rule out potential off-target effects due to CRISPR/Cas9 based genetic mutation or knockout. This is a limitation of our study. However, in analyzing our gRNA sequences (using CRISPOR gRNA design), we have determined that the top 3 potential off-targets for a majority of the sequences are within introns or intergenic regions of the genome. These off-target regions differ in 3 to 4 base pairs from the original gRNA sequence. This suggests that any off-target effects that may result in structural or behavioral changes involved with hippocampal function is low. It remains to be established whether the removal of GPR75 affects the ensembles of hippocampal neurons necessary for contextual retrieval (Dimsdale-Zucker et al. 2022).

Our data show that KO males but not females exhibit an increase in body weight. However, our study was not powered to detect sex differences in the anxiety behavior that could include the body weight as a confounding factor. This is a limitation of our study. Although, it is important to point out that the increase in body weight seen in GPR75 KO male mice was observed when these animals were at least in 26 old weeks, whereas the anxiety behavior was detected as early as at 12 weeks of age. Another limitation of our study is that we have investigated the potential role that GPR75 could play in the brain by focusing on the hippocampus. While our data suggest a potential role for GPR75 in proper function of the hippocampus, we cannot rule out additional functions based on data showing that this receptor is expressed in various brain areas (Uhlen et al. 2015), including the hypothalamus,

Author Manuscript Author Manuscript Author Manuscript Author Manuscript

an important region for feeding and metabolic regulation. In fact, GPR75 appears to regulate energy balance and obesity (Akbari et al. 2021). Thus, it will be important in the near future to expand our investigation to the hypothalamus, a brain area that has been demonstrated to contribute to sexual dimorphisms in energy balance (Tramunt et al. 2020, Gonzalez-Garcia et al. 2023).

The proposed neuronal function of GPR75 may be at odds with the known role of CCL5, one of the ligands for GPR75 (Ignatov et al. 2006, Dedoni et al. 2018). This chemokine is a small protein of 68 amino acids that plays a role in the migration of immune cells across the blood brain barrier to sites of inflammation (Ubogu et al. 2006). However, we have previously shown that CCL5 is constitutively expressed in neurons as well as in non-neuronal cells of the adult rat brain (Lanfranco et al. 2017), where it exerts a neuroprotective activity (Campbell et al. 2015). Most importantly, we observed that similarly to GPR75 mRNA, CCL5 mRNA is expressed in various cells even without injury or inflammation (Lanfranco et al. 2017). Thus, in the adult brain, GPR75/CCL5 signaling may play a role in neuronal transmission. CCL5 signaling was also shown to play a critical period for linking memories through time (Shen et al. 2022). In concert with this suggestion, we propose that GPR75 may respond to constitutive neural release of CCL5 to support a baseline capacity for establishing these linked memories. This is not wholly unexpected because CCL5, like other chemokines (Banisadr et al. 2003), has been suggested to have a role as neuromodulators in the adult brain (Rostene et al. 2007). We also selected the age of the rodents in these experiments to correspond roughly to young adulthood in humans. Use of mice in this age range may mask more profound and important roles for GPR75 in age-related neurological processes. Moreover, restricting our study to young adulthood limits our ability to assess a role for GPR75 in neurodevelopmental processes, a collection of functions to which GPR75 is well-suited to contribute due to its engagement of anti-apoptotic pathways. Extending our research in these directions is likely to provide intriguing new insights into GPR75 within the CNS.

In this study we have used TMT-proteomics to analyzed the difference in protein profile between WT and GPR75 KO mice to reveal potential mechanisms underlying the altered behavior. We have identified a network of proteins that are decreased in the hippocampus of GPR75 KO mice including synapsin I and II, and synaptoporin. Western blot analyses have confirmed a significant decrease of synapsin II and lower levels of synapsin I in GPR75 KO mice. Synapsins and synaptoporin are all synaptic proteins crucial for synaptic structures (Greengard et al. 1993, Murrey et al. 2006, Rosahl et al. 1993). In particular, synapsins contribute to the formation of synapses and synaptic vesicles (Rosahl et al. 1995, Park et al. 2021). In addition, synapsins controls the initial steps of exocytosis that regulate neurotransmitter release (Hilfiker et al. 1999). Thus, a decrease in synapsins observed in GPR75 KO mice could impair the release of neurotransmitters that are involved in hippocampal-dependent memory.

Our study employs an animal model with constitutive lack of GPR75 to elucidate the role of this GPCR in the CNS. Due to the limited published research to date with GPR75 knock-outs, it is difficult to assess our results in light of both known and emerging roles for this receptor. Several studies have identified the eicosanoid 20-HETE as a ligand for GPR75

Author Manuscript Author Manuscript Author Manuscript Author Manuscript

(Fan & Roman 2017, Cardenas et al. 2020, Pascale et al. 2021). This ligand is a potent vasoconstrictor for cerebral arteries; therefore, it is targeted for the development of drugs to reduce infarct volume after ischemic injury (Marumo et al. 2010, Gonzalez-Fernandez et al. 2020, Yi et al. 2016). Our lab has shown that CCL5 promotes GPR75-downstream signaling in neuronal cultures (Dedoni et al. 2018); nevertheless, we cannot exclude that 20-HETE may activate GPR75 in the CNS, especially in specialized limbic structures. However, a different role for GPR75 in the CNS should not be surprising because there are ample examples of receptors mediating metabolic effects in the peripheral system but neuronal effects in the brain. For instance, activation of peripheral noradrenergic receptors promotes glycogenolysis and gluconeogenesis in addition to lipolysis, while in the CNS these receptors play a role in synaptic transmission, wakefulness and arousal (Hussain et al. 2022).

Earlier studies have shown that CCL5 is neuroprotective against amyloid beta (Bruno et al. 2000) or other neurotoxins, including the human immunodeficiency virus protein gp120 (Dedoni et al. 2018, Kaul et al. 2007). However, CCL5, through CCR5, can also exacerbate stroke-induced neurodegeneration (Joy et al. 2019). These data pose the scenario that CCL5 could be neurotoxic or neuroprotective depending upon which cognate receptor it activates. While CCL5 exerts inflammatory functions through CCR5, activation of neuronal GPR75 may serve to protect neurons against gp120 or other neurotoxins. The putative neuroprotective role for GPR75 suggests that GPR75 may serve as a protective factor against acute or chronic CNS insults, especially ones in which CCL5 expression is upregulated as part of a broader pro-neuroinflammatory response. This suggestion is supported by our data showing that GPR75 KO animals exhibit a decrease in synaptic proteins. GPR75 may also act to initiate or sustain neuro-regenerative properties after neural injury. It was recently reported that application of ciliary neurotrophic factor in a model of optic nerve crush injury stimulated CCL5 release and promoted optic nerve regeneration (Xie et al. 2021). GPR75 is known to be highly expressed in retinal tissue (Sauer et al. 2001) and may mediate the pro-regenerative effects of CCL5 in this model. Increasing research attention to the GPR75 signaling as a protective factor in neural injury will enhance our understanding of this GPCR’s role in health and disease and may aid in the future development of GPR75-targeted pharmacotherapies.

Supplementary Material

Refer to Web version on PubMed Central for supplementary material.

Acknowledgements.

This work was supported by President Award for Distinguished Scholar-Teachers, Georgetown University, the National Institute of Health grants R01 NS079172 to IM, and T32 041218 to AS. BCM Mass Spectrometry Proteomics Core is supported by the Dan L. Duncan Comprehensive Cancer Center Award (P30 CA125123), CPRIT Core Facility Awards (RP170005 and RP210227), Intellectual Developmental Disabilities Research Center Award (P50 HD103555), and NIH High End Instrument award (S10 OD026804, Orbitrap Exploris 480).

Author Manuscript Author Manuscript Author Manuscript Author Manuscript

Data availability.

The dataset used and/or analyzed during the current study are available from the corresponding author. GPR75 KO mice will be available upon reasonable request.

Abbreviations used are:

ANOVA	analysis of variance
BSA	bovine serum albumin
CNS	central nervous system
CS	conditional stimulus
GFAP	glial fibrillary acidic protein
GPCRs	G-protein coupled receptors
GPR75	G-protein coupled receptor 75
HPLC	High-performance liquid chromatography
KO	knockout
Iba-1	ionized calcium binding adaptor molecule-1= number of animals used
NeuN	neuronal nuclear antigen
PBS	phosphate buffered saline
PCR	Polymerase Chain Reaction
RbFox3	RNA binding protein Fox-3
RT	room temperature
RT-PCR	Reverse Transcriptase-PCR
SEM	standard error of the mean
TAE	Tris-acetate-ethylenediaminetetraacetic acid
TEAB	Triethylammonium bicarbonate
TMT	Tandem Mass Tag
WT	wild type
20-HETE	20-Hydroxyeicosatetraenoic acid

Author Manuscript Author Manuscript Author Manuscript Author Manuscript

References

Akbari P, Gilani A, Sosina O et al. (2021) Sequencing of 640,000 exomes identifies GPR75 variants associated with protection from obesity. Science, 373.

Bachis A, Wenzel E, Boelk A, Becker J and Mocchetti I (2016) The neurotrophin receptor p75 mediates gp120-induced loss of synaptic spines in aging mice. Neurobiol Aging, 46, 160–168. [PubMed: 27498053]

Banisadr G, Skrzydelski D, Kitabgi P, Rostene W and Parsadaniantz SM (2003) Highly regionalized distribution of stromal cell-derived factor-1/CXCL12 in adult rat brain: constitutive expression in cholinergic, dopaminergic and vasopressinergic neurons. Eur J Neurosci, 18, 1593–1606. [PubMed: 14511338]

Bruno V, Copani A, Besong G, Scoto G and Nicoletti F (2000) Neuroprotective activity of chemokines against N-methyl-D-aspartate or beta-amyloid-induced toxicity in culture. Eur J Pharmacol, 399, 117–121. [PubMed: 10884510]

Campbell LA, Avdoshina V, Day C, Lim ST and Mocchetti I (2015) Pharmacological induction of CCL5 in vivo prevents gp120-mediated neuronal injury. Neuropharmacology, 92, 98–107. [PubMed: 25623966]

Cardenas S, Colombero C, Panelo L, Dakarapu R, Falck JR, Costas MA and Nowicki S (2020) GPR75 receptor mediates 20-HETE-signaling and metastatic features of androgen-insensitive prostate cancer cells. Biochim Biophys Acta Mol Cell Biol Lipids, 1865, 158573. [PubMed: 31760076]

Carr DB, Day M, Cantrell AR, Held J, Scheuer T, Catterall WA and Surmeier DJ (2003) Transmitter modulation of slow, activity-dependent alterations in sodium channel availability endows neurons with a novel form of cellular plasticity. Neuron, 39, 793–806. [PubMed: 12948446]

Chambers MC, Maclean B, Burke R et al. (2012) A cross-platform toolkit for mass spectrometry and proteomics. Nat Biotechnol, 30, 918–920. [PubMed: 23051804]

Civelli O (2012) Orphan GPCRs and neuromodulation. Neuron, 76, 12–21. [PubMed: 23040803]

Civelli O, Reinscheid RK, Zhang Y, Wang Z, Fredriksson R and Schioth HB (2013) G protein-coupled receptor deorphanizations. Annu Rev Pharmacol Toxicol, 53, 127–146. [PubMed: 23020293]

Dedoni S, Campbell LA, Harvey BK, Avdoshina V and Mocchetti I (2018) The Orphan G Protein-coupled Receptor 75 Signaling is Activated by the Chemokine CCL5. J Neurochem.

Dimsdale-Zucker HR, Montchal ME, Reagh ZM, Wang SF, Libby LA and Ranganath C (2022) Representations of Complex Contexts: A Role for Hippocampus. J Cogn Neurosci, 1–21.

Doze VA and Perez DM (2012) G-Protein-Coupled Receptors in Adult Neurogenesis. Pharmacological Reviews, 64, 645–675. [PubMed: 22611178]

Fan F and Roman RJ (2017) GPR75 Identified as the First 20-HETE Receptor: A Chemokine Receptor Adopted by a New Family. Circ Res, 120, 1696–1698. [PubMed: 28546348]

Garcia V, Gilani A, Shkolnik B et al. (2017) 20-HETE Signals Through G-Protein-Coupled Receptor GPR75 (Gq) to Affect Vascular Function and Trigger Hypertension. Circ Res, 120, 1776–1788. [PubMed: 28325781]

Gilani A, Agostinucci K, Hossain S, Pascale JV, Garcia V, Adebesin AM, Falck JR and Schwartzman ML (2021) 20-HETE interferes with insulin signaling and contributes to obesity-driven insulin resistance. Prostaglandins Other Lipid Mediat, 152, 106485. [PubMed: 33011364]

Gonzalez-Fernandez E, Staursky D, Lucas K et al. (2020) 20-HETE Enzymes and Receptors in the Neurovascular Unit: Implications in Cerebrovascular Disease. Front Neurol, 11, 983. [PubMed: 33013649]

Gonzalez-Garcia I, Garcia-Clave E, Cebrian-Serrano A et al. (2023) Estradiol regulates leptin sensitivity to control feeding via hypothalamic Cited1. Cell Metab, 35, 438–455 e437. [PubMed: 36889283]

Greengard P, Valtorta F, Czernik AJ and Benfenati F (1993) Synaptic vesicle phosphoproteins and regulation of synaptic function. Science, 259, 780–785. [PubMed: 8430330]

Gu Z, Eils R and Schlesner M (2016) Complex heatmaps reveal patterns and correlations in multidimensional genomic data. Bioinformatics, 32, 2847–2849. [PubMed: 27207943]

Author Manuscript Author Manuscript Author Manuscript Author Manuscript

Hilfiker S, Pieribone VA, Czernik AJ, Kao HT, Augustine GJ and Greengard P (1999) Synapsins as regulators of neurotransmitter release. Philos Trans R Soc Lond B Biol Sci, 354, 269–279. [PubMed: 10212475]

Hochberg Y and Benjamini Y (1990) More powerful procedures for multiple significance testing. Stat Med, 9, 811–818. [PubMed: 2218183]

Hussain LS, Reddy V and Maani CV (2022) Physiology, Noradrenergic Synapse. In: StatPearls. Treasure Island (FL).

Ignatov A, Robert J, Gregory-Evans C and Schaller HC (2006) RANTES stimulates Ca2+ mobilization and inositol trisphosphate (IP3) formation in cells transfected with G protein-coupled receptor 75. Br J Pharmacol, 149, 490–497. [PubMed: 17001303]

Johnson WE, Li C and Rabinovic A (2007) Adjusting batch effects in microarray expression data using empirical Bayes methods. Biostatistics, 8, 118–127. [PubMed: 16632515]

Joy MT, Ben Assayag E, Shabashov-Stone D et al. (2019) CCR5 Is a Therapeutic Target for Recovery after Stroke and Traumatic Brain Injury. Cell, 176, 1143–1157 e1113. [PubMed: 30794775]

Kaul M, Ma Q, Medders KE, Desai MK and Lipton SA (2007) HIV-1 coreceptors CCR5 and CXCR4 both mediate neuronal cell death but CCR5 paradoxically can also contribute to protection. Cell Death Differ, 14, 296–305. [PubMed: 16841089]

Kempf A, Tews B, Arzt ME et al. (2014) The Sphingolipid Receptor S1PR2 Is a Receptor for Nogo-A Repressing Synaptic Plasticity. Plos Biology, 12.

Kong AT, Leprevost FV, Avtonomov DM, Mellacheruvu D and Nesvizhskii AI (2017) MSFragger: ultrafast and comprehensive peptide identification in mass spectrometry-based proteomics. Nat Methods, 14, 513–520. [PubMed: 28394336]

Kurabayashi N, Nguyen MD and Sanada K (2013) The G protein-coupled receptor GPRC5B contributes to neurogenesis in the developing mouse neocortex. Development, 140, 4335–4346. [PubMed: 24089469]

Lanfranco MF, Mocchetti I, Burns MP and Villapol S (2017) Glial- and Neuronal-Specific Expression of CCL5 mRNA in the Rat Brain. Front Neuroanat, 11, 137. [PubMed: 29375328]

Leek JT, Johnson WE, Parker HS, Jaffe AE and Storey JD (2012) The sva package for removing batch effects and other unwanted variation in high-throughput experiments. Bioinformatics, 28, 882–883. [PubMed: 22257669]

Lievens JC, Woodman B, Mahal A and Bates GP (2002) Abnormal phosphorylation of synapsin I predicts a neuronal transmission impairment in the R6/2 Huntington's disease transgenic mice. Mol Cell Neurosci, 20, 638–648. [PubMed: 12213445]

Liu B, Hassan Z, Amisten S, King AJ, Bowe JE, Huang GC, Jones PM and Persaud SJ (2013) The novel chemokine receptor, G-protein-coupled receptor 75, is expressed by islets and is coupled to stimulation of insulin secretion and improved glucose homeostasis. Diabetologia, 56, 2467–2476. [PubMed: 23979485]

Lugo JN, Smith GD and Holley AJ (2014) Trace Fear Conditioning in Mice. Jove-Journal of Visualized Experiments.

Luo R, Jeong SJ, Jin ZH, Strokes N, Li SH and Piao XH (2011) G protein-coupled receptor 56 and collagen III, a receptor-ligand pair, regulates cortical development and lamination. Proceedings of the National Academy of Sciences of the United States of America, 108, 12925–12930. [PubMed: 21768377]

Marumo T, Eto K, Wake H, Omura T and Nabekura J (2010) The inhibitor of 20-HETE synthesis, TS-011, improves cerebral microcirculatory autoregulation impaired by middle cerebral artery occlusion in mice. Br J Pharmacol, 161, 1391–1402. [PubMed: 20735406]

Matas-Rico E, Garcia-Diaz B, Llebrez-Zayas P et al. (2008) Deletion of lysophosphatidic acid receptor LPA(1) reduces neurogenesis in the mouse dentate gyrus. Molecular and Cellular Neuroscience, 39, 342–355. [PubMed: 18708146]

Monroe ME, Shaw JL, Daly DS, Adkins JN and Smith RD (2008) MASIC: a software program for fast quantitation and flexible visualization of chromatographic profiles from detected LC-MS(/MS) features. Comput Biol Chem, 32, 215–217. [PubMed: 18440872]

Author Manuscript Author Manuscript Author Manuscript Author Manuscript

Murrey HE, Gama CI, Kalovidouris SA, Luo WI, Driggers EM, Porton B and Hsieh-Wilson LC (2006) Protein fucosylation regulates synapsin Ia/Ib expression and neuronal morphology in primary hippocampal neurons. Proc Natl Acad Sci U S A, 103, 21–26. [PubMed: 16373512]

Park D, Wu Y, Lee SE, Kim G, Jeong S, Milovanovic D, De Camilli P and Chang S (2021) Cooperative function of synaptophysin and synapsin in the generation of synaptic vesicle-like clusters in non-neuronal cells. Nat Commun, 12, 263. [PubMed: 33431828]

Pascale JV, Park EJ, Adebesin AM, Falck JR, Schwartzman ML and Garcia V (2021) Uncovering the signalling, structure and function of the 20-HETE-GPR75 pairing: Identifying the chemokine CCL5 as a negative regulator of GPR75. Br J Pharmacol, 178, 3813–3828. [PubMed: 33974269]

Powell DR, Doree DD, DaCosta CM, Platt KA, Brommage R, Buhring L, Revelli JP and Shadoan MK (2022) Mice Lacking Gpr75 are Hypophagic and Thin. Diabetes Metab Syndr Obes, 15, 45–58. [PubMed: 35023939]

Ritchie ME, Phipson B, Wu D, Hu Y, Law CW, Shi W and Smyth GK (2015) limma powers differential expression analyses for RNA-sequencing and microarray studies. Nucleic Acids Res, 43, e47. [PubMed: 25605792]

Rosahl TW, Geppert M, Spillane D, Herz J, Hammer RE, Malenka RC and Sudhof TC (1993) Short-term synaptic plasticity is altered in mice lacking synapsin I. Cell, 75, 661–670. [PubMed: 7902212]

Rosahl TW, Spillane D, Missler M, Herz J, Selig DK, Wolff JR, Hammer RE, Malenka RC and Sudhof TC (1995) Essential functions of synapsins I and II in synaptic vesicle regulation. Nature, 375, 488–493. [PubMed: 7777057]

Rostene W, Kitabgi P and Parsadaniantz SM (2007) Chemokines: a new class of neuromodulator? Nat Rev Neurosci, 8, 895–903. [PubMed: 17948033]

Saltzman AB, Leng M, Bhatt B et al. (2018) gpGrouper: A Peptide Grouping Algorithm for Gene-Centric Inference and Quantitation of Bottom-Up Proteomics Data. Mol Cell Proteomics, 17, 2270–2283. [PubMed: 30093420]

Sanderson TM, Hogg EL, Collingridge GL and Correa SAL (2016) Hippocampal metabotropic glutamate receptor long-term depression in health and disease: focuson mitogen-activated protein kinase pathways. Journal of Neurochemistry, 139, 200–214. [PubMed: 26923875]

Sauer CG, White K, Stohr H et al. (2001) Evaluation of the G protein coupled receptor-75 (GPR75) in age related macular degeneration. Br J Ophthalmol, 85, 969–975. [PubMed: 11466257]

Shen Y, Zhou M, Cai D et al. (2022) CCR5 closes the temporal window for memory linking. Nature, 606, 146–152. [PubMed: 35614219]

Sjostedt E, Zhong W, Fagerberg L et al. (2020) An atlas of the protein-coding genes in the human, pig, and mouse brain. Science, 367.

Speidell A, Asuni GP, Avdoshina V, Scognamiglio S, Forcelli P and Mocchetti I (2019) Reversal of Cognitive Impairment in gp120 Transgenic Mice by the Removal of the p75 Neurotrophin Receptor. Front Cell Neurosci, 13, 398. [PubMed: 31543761]

Speidell A, Asuni GP, Wakulski R and Mocchetti I (2020) Up-regulation of the p75 neurotrophin receptor is an essential mechanism for HIV-gp120 mediated synaptic loss in the striatum. Brain Behav Immun, 89, 371–379. [PubMed: 32717404]

Tarttelin EE, Kirschner LS, Bellingham J, Baffi J, Taymans SE, Gregory-Evans K, Csaky K, Stratakis CA and Gregory-Evans CY (1999) Cloning and characterization of a novel orphan G-protein-coupled receptor localized to human chromosome 2p16. Biochem Biophys Res Commun, 260, 174–180. [PubMed: 10381362]

Tramunt B, Smati S, Grandgeorge N, Lenfant F, Arnal JF, Montagner A and Gourdy P (2020) Sex differences in metabolic regulation and diabetes susceptibility. Diabetologia, 63, 453–461. [PubMed: 31754750]

Ubogu EE, Callahan MK, Tucky BH and Ransohoff RM (2006) Determinants of CCL5-driven mononuclear cell migration across the blood “brain barrier. Implications for therapeutically modulating neuroinflammation. J Neuroimmunol, 179, 132–144. [PubMed: 16857269]

Uhlen M, Fagerberg L, Hallstrom BM et al. (2015) Proteomics. Tissue-based map of the human proteome. Science, 347, 1260419. [PubMed: 25613900]

Author Manuscript Author Manuscript Author Manuscript Author Manuscript

White LO, Bywater MJ, Lovering AM, Holt HA and Reeves DS (1988) Chloramphenicol assay by EMIT. J Antimicrob Chemother, 21, 683–684. [PubMed: 3292501]

Wiltgen BJ, Sanders MJ, Ferguson C, Homanics GE and Fanselow MS (2005) Trace fear conditioning is enhanced in mice lacking the delta subunit of the GABAA receptor. Learn Mem, 12, 327–333. [PubMed: 15897254]

Wootten D, Christopoulos A, Marti-Solano M, Babu MM and Sexton PM (2018) Mechanisms of signalling and biased agonism in G protein-coupled receptors. Nat Rev Mol Cell Biol, 19, 638–653. [PubMed: 30104700]

Xie L, Yin Y and Benowitz L (2021) Chemokine CCL5 promotes robust optic nerve regeneration and mediates many of the effects of CNTF gene therapy. Proc Natl Acad Sci U S A, 118.

Yi X, Han Z, Zhou Q, Lin J and Liu P (2016) 20-Hydroxyeicosatetraenoic Acid as a Predictor of Neurological Deterioration in Acute Minor Ischemic Stroke. Stroke, 47, 3045–3047. [PubMed: 27834744]

Author Manuscript Author Manuscript Author Manuscript Author Manuscript

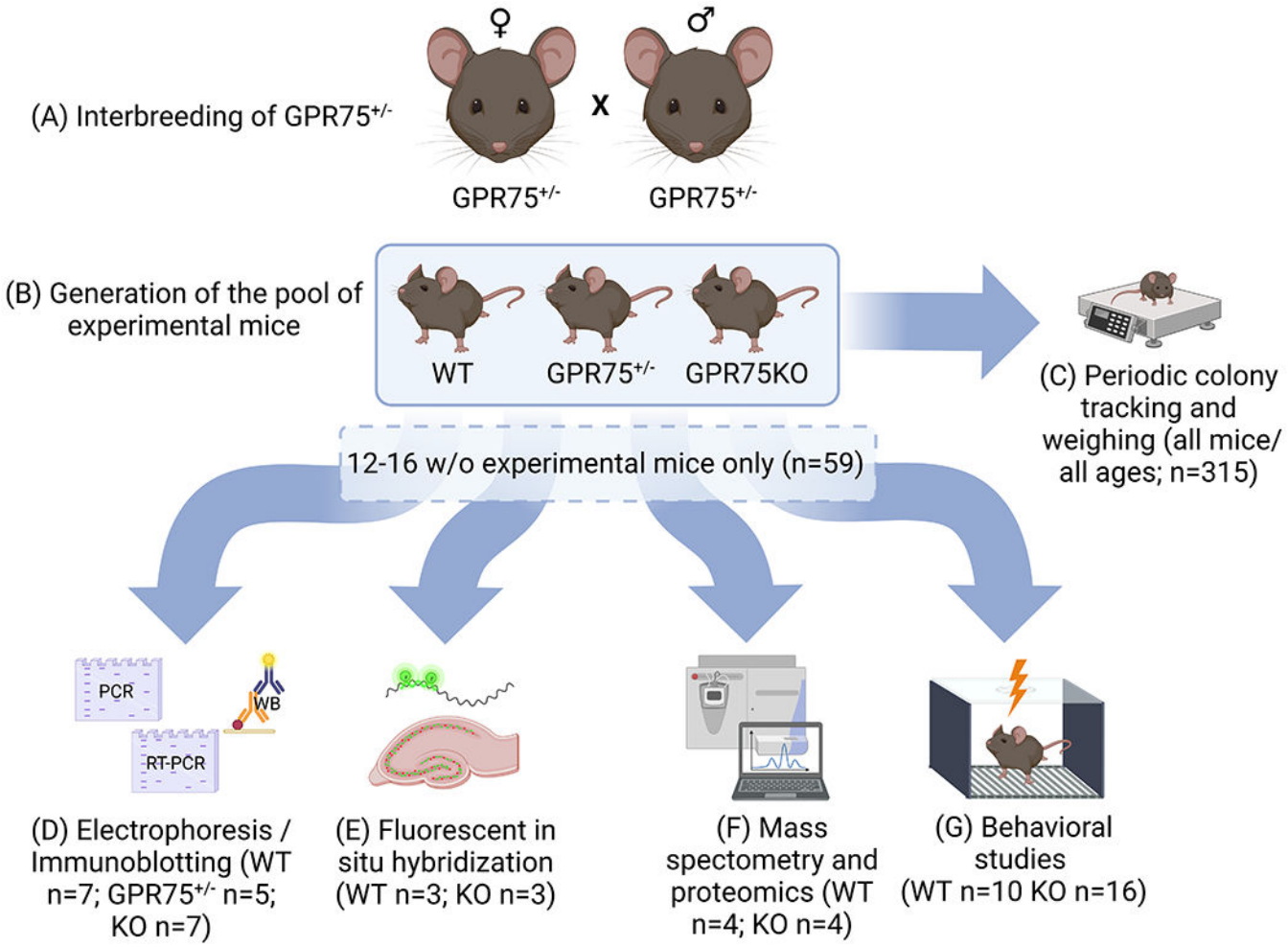

Figure 1. Timeline outlining experimental design and animal groups.

A. Multiple pairs of GPR75 heterozygotes were interbred to generate the colony of mice available for experiments. **B** and **C.** From this pool, separate cohorts of mice were weighed at 12 and 26 weeks old (w/o) and returned to the total pool of experimental mice. Experimental mice for this series of experiments (n=58) were arbitrarily assigned to one of four endpoints in this study in roughly equal numbers of wild type (WT) or knockout (KO): **D.** electrophoresis and immunoblotting, **E.** RNAScope® / fluorescent *in situ* hybridization, **F.** mass spectrometry-based proteomics, or **G.** behavioral testing.

Author Manuscript Author Manuscript Author Manuscript Author Manuscript

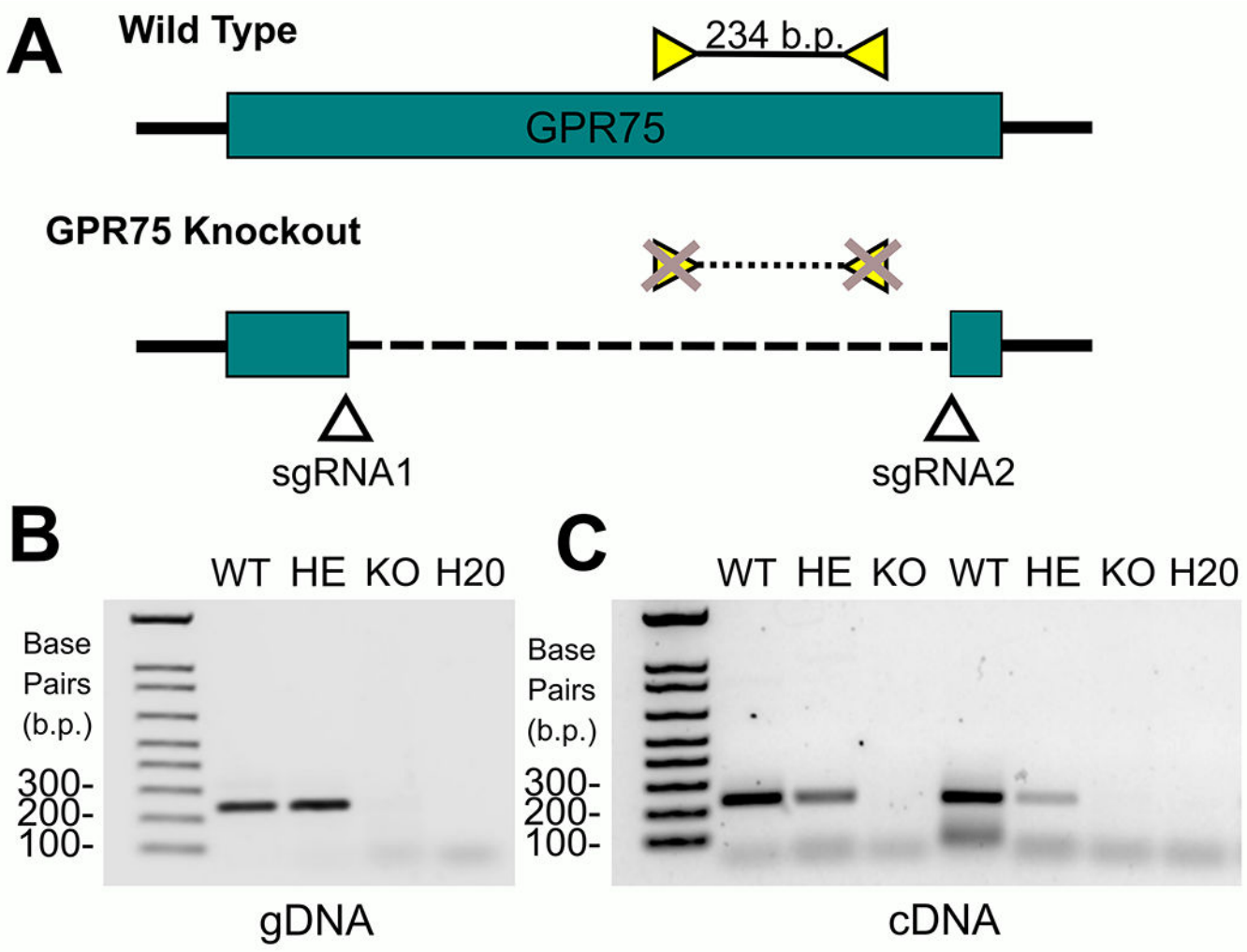

Figure 2. Polymerase chain reaction confirmation of knockout in GPR75$^{-/-}$ mutant mice

A. Schematic diagram of GPR75 genomic DNA where the GPR75 deletion is indicated by the dashed line. **B**. Polymerase chain reaction (PCR) on genomic DNA extracted from WT, GPR75$^{+/-}$ (HE), and GPR75$^{-/-}$ (KO) cerebellar tissue, which were normalized to 50 ng per lane. The loading control was UltraPure Water. Results represent treatment with primer pairs indicated in A. **C.** PCR on complementary mRNA extracted from wild type (WT), heterozygous (HE), and GPR75 knockout (KO) cerebral tissue, which were normalized to 300 ng per lane. The loading control was UltraPure Water.

Author Manuscript Author Manuscript Author Manuscript Author Manuscript

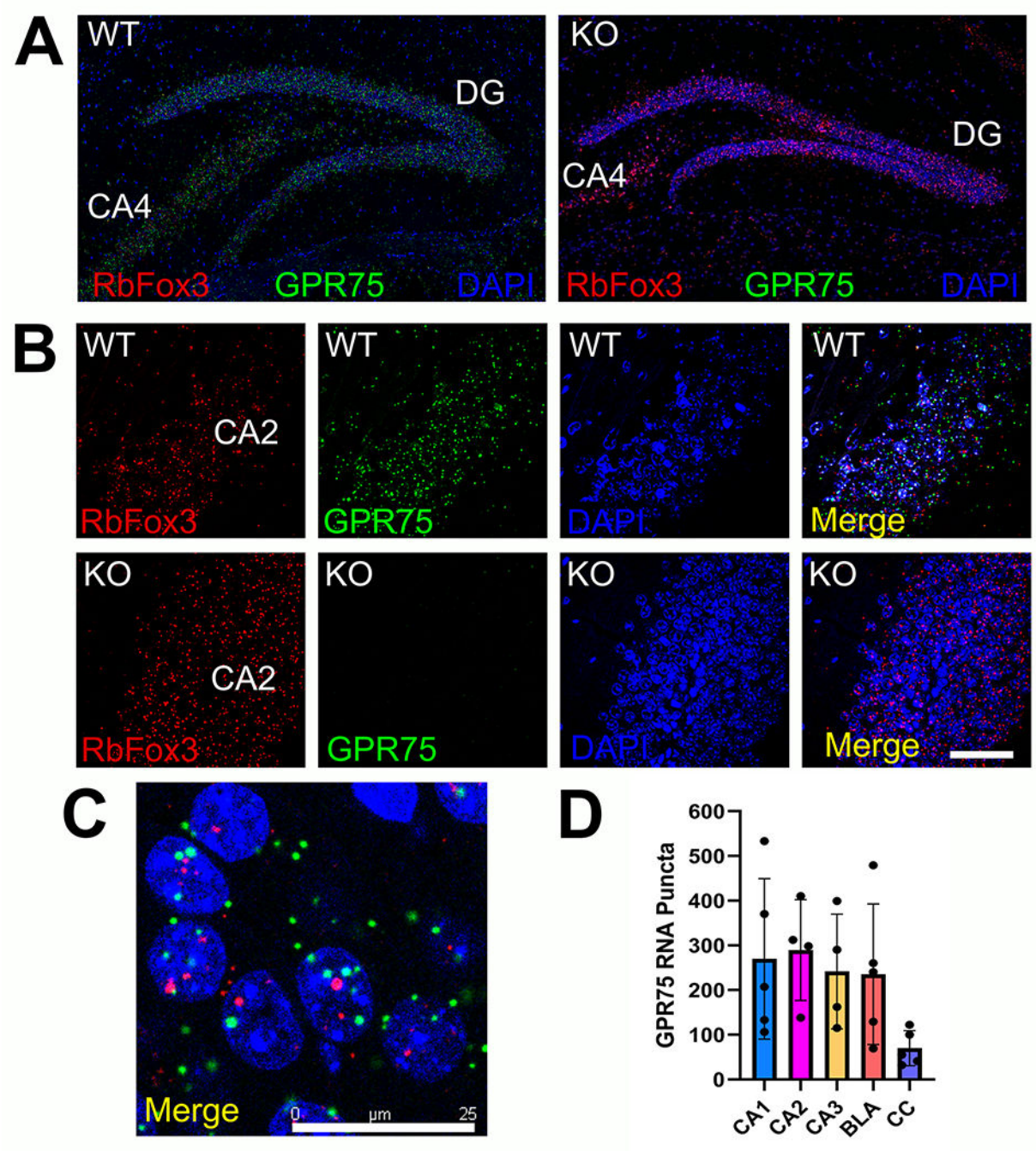

Figure 3. Expression of GPR75 mRNA in adult mice.

GPR75 mRNA was detected in adult mouse brain by RNAscope. **A**. The probe for GPR75 was first validated in the hippocampus of wild type (WT) and GPR75 null (KO) mice. Please note the absence of GPR75 puncta (green) in KO animals. RbFox 3 mRNA (red) was used to visualize neurons, DAPI (blue) was used to identify cell bodies. **B**. Representative images for RbFox3 (red) and GPR75 (green) mRNAs in the hippocampus of WT and KO mice. DAPI (blue) was used to visualize nuclei. Scale bar= 50 µm. **C**. Representative high magnification of a hippocampal section through the CA1 region used to quantify puncta. **D**.

Author Manuscript Author Manuscript Author Manuscript Author Manuscript

Quantifications of GPR75 mRNA puncta within neurons were performed on a series of 5 randomly selected coronal sections per mice, from a total of 3 mice per group, throughout the hippocampus (CA1-CA3), basolateral amygdala (BLA) and corpus callosum (CC). Data, presented as the mean ± SEM, are expressed as the average of double-stained cells per section per animal.

Author Manuscript Author Manuscript Author Manuscript Author Manuscript

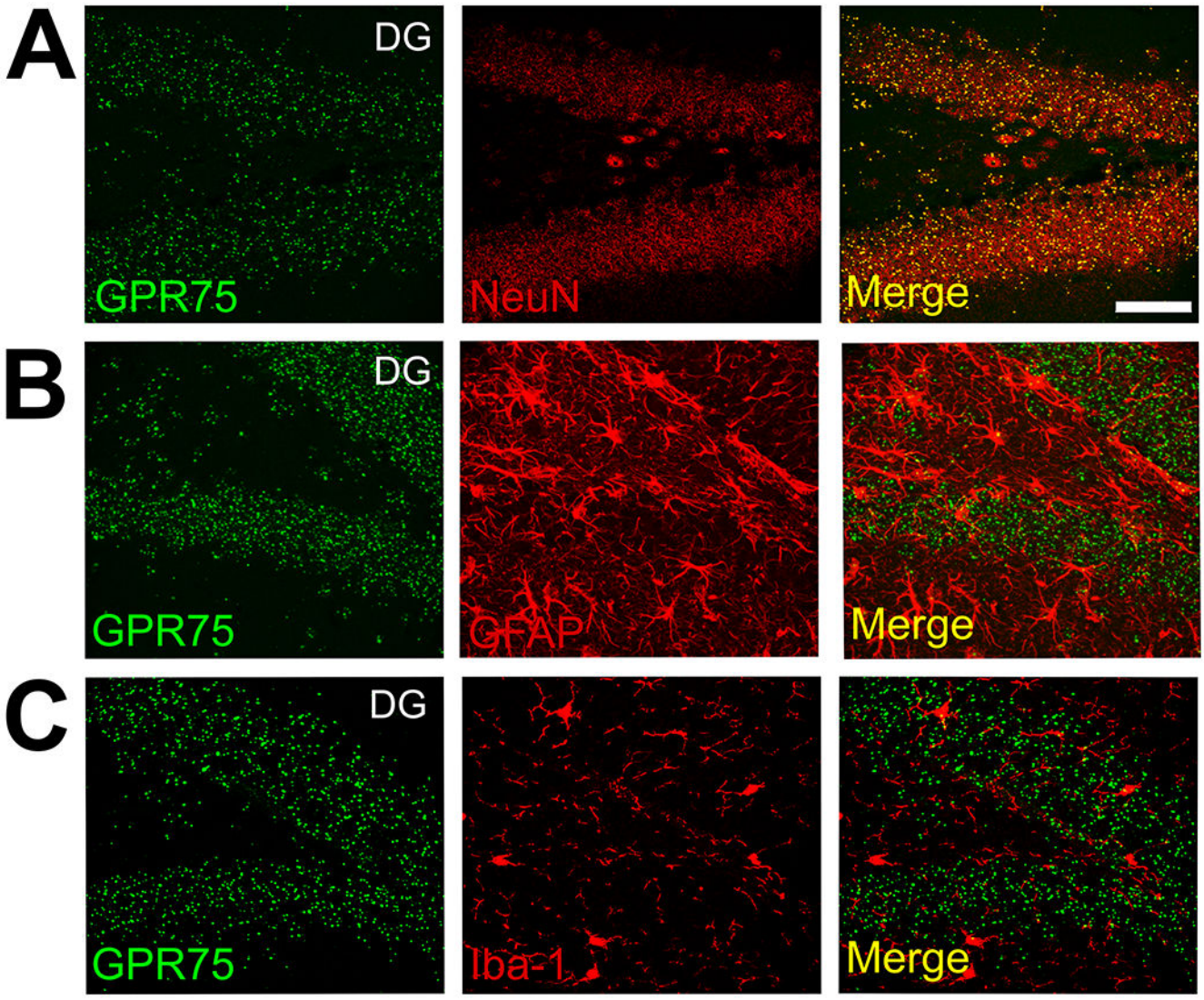

Figure 4. Expression of GPR75 mRNA is confined to neurons.

RNAscope and immunohistochemistry were used to identify which cells in adult mouse dentate gyrus (DG) express GPR75 mRNA. **A**. Representative images for GPR75 mRNA (green) and NeuN (red) immunohistochemistry. Merge shows a number of yellow (red+green) puncta denoting colocalization of GPR75 within neurons. **B** and **C**. After RNAscope for GPR75 mRNA, hippocampal sections were stained for glial fibrillary acidic protein (GFAP) or ionized calcium binding adaptor molecule-1 (Iba-1), respectively. Merge images show no GPR75 mRNA in astrocytes or microglial cells (from a total of 5 randomly selected coronal sections per mice, from a total of 3 mice). Scale bar=50 μm.

Author Manuscript Author Manuscript Author Manuscript Author Manuscript

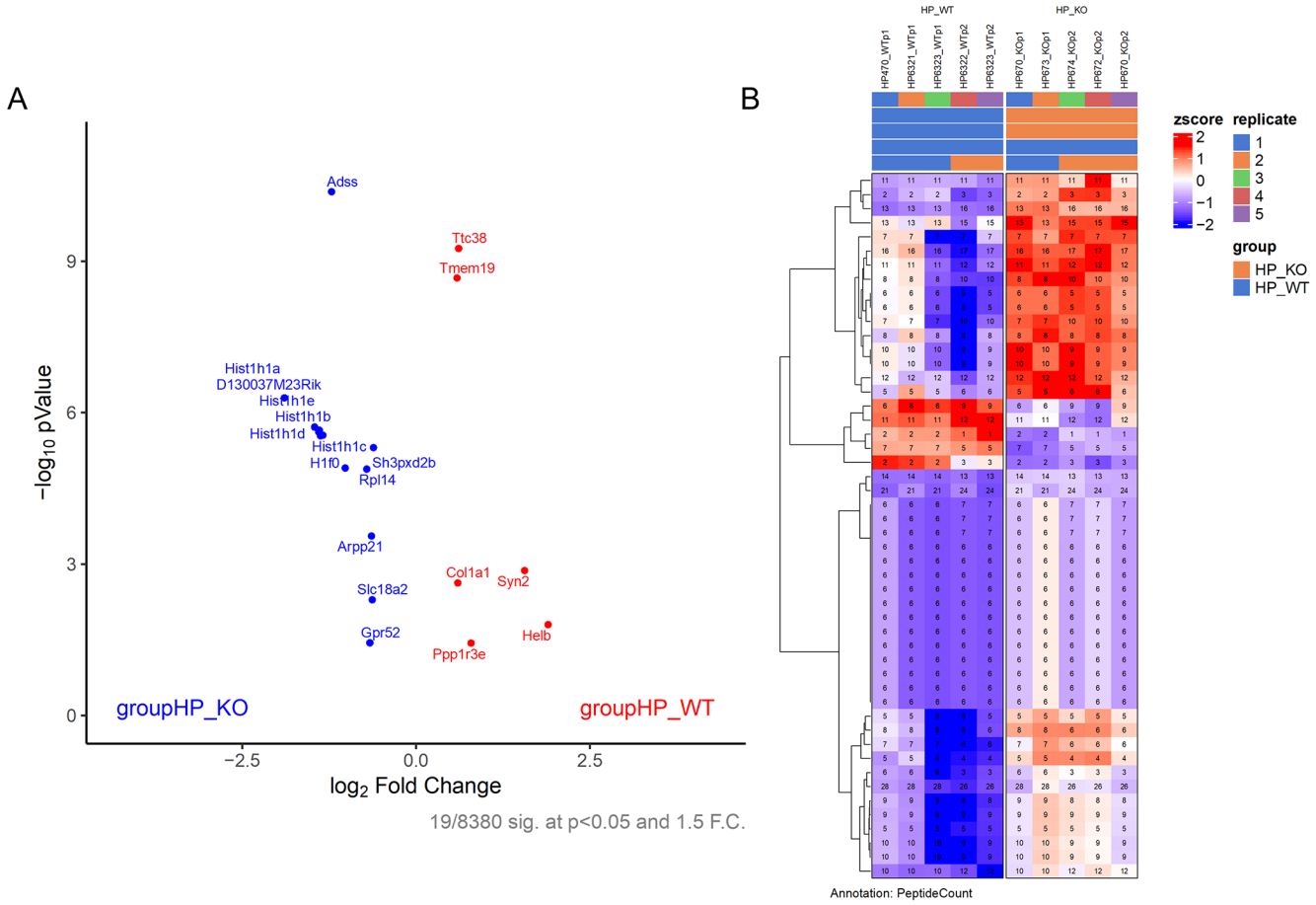

Figure 5. Tandem Mass Tag (TMT) protein co-expression network.

The hippocampi from wildtype (WT) and GPR75 Knockout (KO) mice (n = 4, each group) were analyzed by tandem mass tag (TMT)-Mass spectrometry-based proteomics. After outlier removal and data processing, a total of 8,980 proteins were analyzed by significant changes in expression. **A.** Log_2 fold change summarizes ratios of protein changes in WT versus GPR75 KO mice. Points above the non-axial horizontal line represent proteins with significantly different abundances ($p < 0.05$). Points to the left most non-axial vertical line denote protein fold changes of GPR75 KO/WT less than −1.5, while points to the right of the right-most non-axial vertical line denote protein fold changes of GPR75 KO/WT greater than 1.5. **B**. Summary of proteins whose changes are affected by the removal of GPR75 in the hippocampus. Heatmap was generated with ComplexHeatmap (Gu et al. 2016).

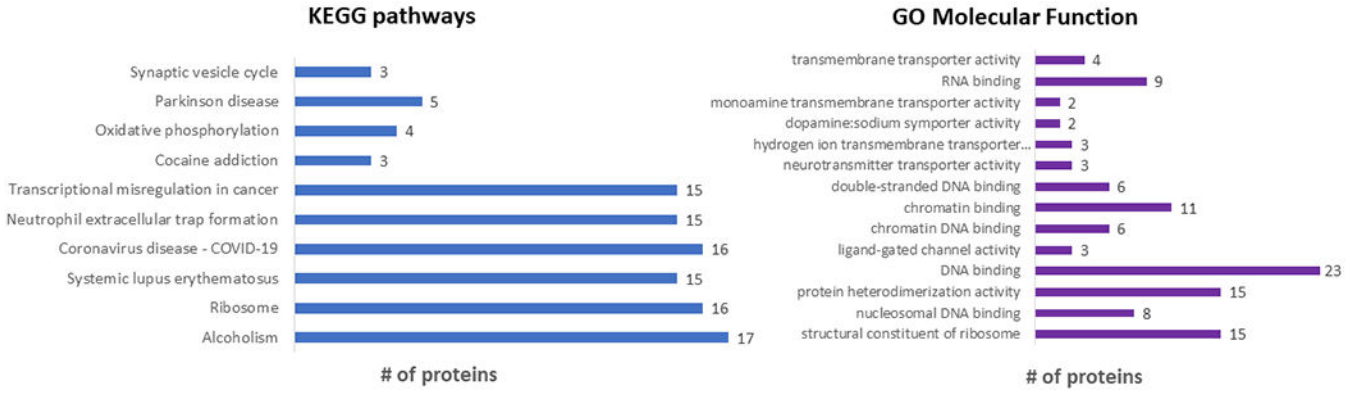

Figure. 6. KEGG pathways enrichment and functional classification of different expressed protein.

The significant enrichments of differentially expressed proteins are represented in this Figure. According to the Kyoto Encyclopedia of Genes and Genomes (KEGG) classification, these differentially expressed molecules were related to the synaptic vesicle cycle that involves synaptic proteins (e.g., synapsin 1 and 2, and synaptoporin). Others pathways out of the interest of the present study including systemic lupus erythematosus, alcoholism, cocaine addictions were also identified.

Author Manuscript Author Manuscript Author Manuscript Author Manuscript

Author Manuscript Author Manuscript Author Manuscript Author Manuscript

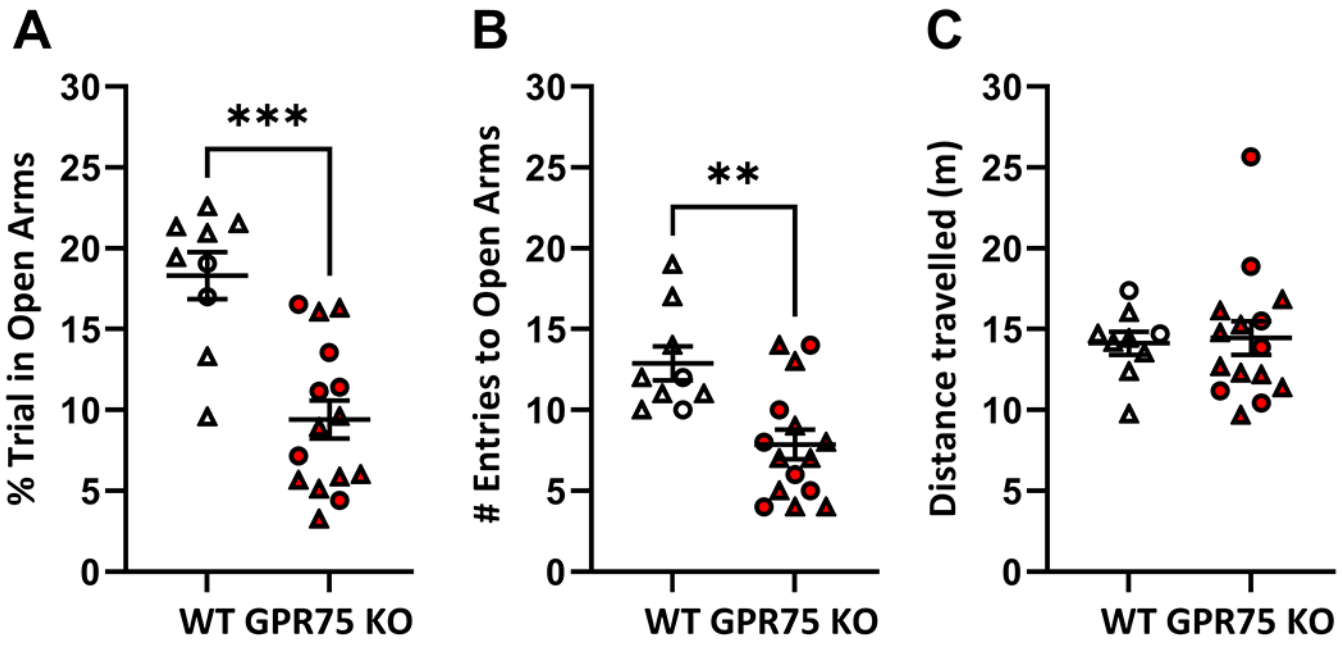

Figure 7. GPR75 knockout mice (KO) display increased anxiety-related behaviors within the elevated plus maze.

Wild type (WT) mice (n=9; 2 females (circle) and 7 males (triangles) spend: (**A)** an increased duration within open arms of the elevated plus maze ($t_{[22]}$=4.722, p<0.001; males only $t_{[14]}$=4.048, p<0.01) and (**B)** undertake a greater number of entries to these arms within a 10-minute trial (U=20, p<0.01; males only U=8.5, p<0.01) when compared to GPR75 KO mice [(n=15; 7 females (circles) and 9 males (triangles)]. **C.** There is no effect for genotype in cumulative spontaneous ambulation within the apparatus ($t_{[22]}$=0.2247, p=0.8243; males only $t_{[14]}$=0.0936, p=0.9268). Student's two-tailed t-test, or two-tailed Mann-Whitney U. *p<0.05, **p<0.01. Data are presented as mean ± SEM.

Author Manuscript Author Manuscript Author Manuscript Author Manuscript

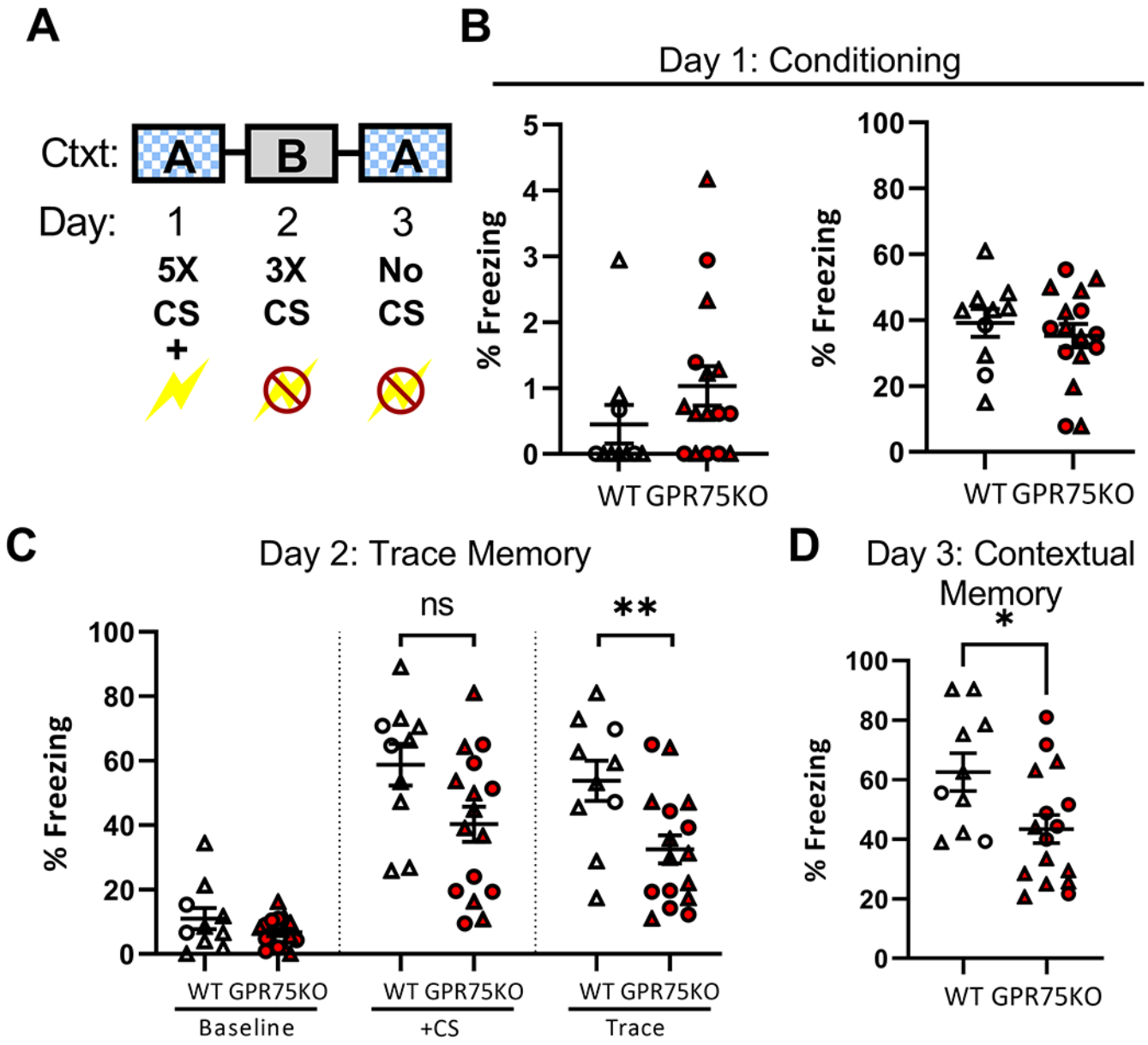

Figure 8. GPR75 knockout mice (KO) are impaired on a trace fear conditioning task.

A. Experimental paradigm. **B-D.** the number of animals used is: WT n=10; 2 females (circles) and 8 males (triangles). GPR75 KO n=16; 7 females (circles) and 9 males (triangles). **B.** Freezing behaviors during baseline and conditioning periods within day 1 are equivalent between genotypes in context A. Baseline (U=51, p=0.11; males only U=51, p=0.09) and conditioning ($t_{[24]}$=0.6854, p = 0.4996; males only $t_{[15]}$=0.7553, p = 0.4618). **C.** GPR75 KO rodents freeze less often than do wild type (WT) mice within the trace period $t_{[24]}$=2.874, p<0.01, males only $t_{[15]}$=2.011, p=0.062) 24 h after conditioning, while retaining comparable levels of baseline (pre-CS) freezing in context B (U=65.50, p=0.4596; males only U=32.50, p=0.7650). **D.** GPR75 KO mice display reduced freezing behavior when reintroduced into context A ($t_{[24]}$=2.452, p<0.05; males only $t_{[15]}$=3.226,

p<0.01). Student's two-tailed t-test, or two-tailed Mann-Whitney U. *p<0.05, **p<0.01 for the indicated groupwise comparison. Data are presented as mean ± SEM.

Author Manuscript Author Manuscript Author Manuscript Author Manuscript

Author Manuscript Author Manuscript Author Manuscript Author Manuscript

Table 1.

List of down-regulated proteins in the hippocampus of GPR75 knockout mice *

GeneID	GeneSymbol	GeneDescription	Fold change hippocampus KO vs WT
11944	Atp4a	ATPase, H+/K+ exchanging, gastric, alpha polypeptide	−1.318161238
12175	Bnip2	BCL2/adenovirus E1B interacting protein 2	−1.277377433
12561	Cdh4	cadherin 4	−1.201366629
12842	Col1a1	collagen, type I, alpha 1	−1.513853886
15199	Hebp1	heme binding protein 1	−1.434468522
16565	Kif21b	kinesin family member 21B	−1.274107526
18515	Pbx2	pre B cell leukemia homeobox 2	−1.226138575
18975	Polg	polymerase (DNA directed), gamma	−1.280084521
20964	Syn1	synapsin I	−1.20016826
20965	Syn2	synapsin II	−2.945602247
23876	Fbln5	fibulin 5	−1.215711956
26570	Slc7a11	solute carrier family 7 (cationic amino acid transporter, y+ system), member 11	−1.238968387
57773	Wdr4	WD repeat domain 4	−1.203131044
65103	Arl6ip6	ADP-ribosylation factor-like 6 interacting protein 6	−1.199670033
65970	Lima1	LIM domain and actin binding 1	−1.370609559
66059	Krtcap2	keratinocyte associated protein 2	−1.340522462
67226	Tmem19	transmembrane protein 19	−1.50239118
67285	Cwc27	CWC27 spliceosome-associated protein homolog (S. cerevisiae)	−1.21459736
67441	Isoc2b	isochorismatase domain containing 2b	−1.280979075
67463	Poc5	POC5 centriolar protein homolog (Chlamydomonas)	−1.362468559
67528	Nudt7	nudix (nucleoside diphosphate linked moiety X)-type motif 7	−1.241019615
69259	Kctd5	potassium channel tetramerisation domain containing 5	−1.229299909
72003	Synpr	synaptoporin	−1.236488827
72269	Cda	cytidine deaminase	−1.245329699
72961	Slc17a7	solute carrier family 17 (sodium-dependent inorganic phosphate cotransporter), member 7	−1.201783581
74777	Sepn1	selenoprotein N, 1	−1.251025101
76411	Ift43	intraflagellar transport 43	−1.207397941
78248	Armcx1	armadillo repeat containing, X-linked 1	−1.215359313
78797	Ndor1	NADPH dependent diflavin oxidoreductase 1	−1.384767223
105651	Ppp1r3e	protein phosphatase 1, regulatory (inhibitor) subunit 3E	−1.72826963
117599	Helb	helicase (DNA) B	−3.726804959
140571	Plxnb3	plexin B3	−1.205979677
217682	Plekhd1	pleckstrin homology domain containing, family D (with coiled-coil domains) member 1	−1.260455864
239570	Ttc38	tetratricopeptide repeat domain 38	−1.527130337

Author Manuscript
Author Manuscript
Author Manuscript
Author Manuscript

GeneID	GeneSymbol	GeneDescription	Fold change hippocampus KO vs WT
243937	Zfp536	zinc finger protein 536	−1.218684721
268752	Wdfy2	WD repeat and FYVE domain containing 2	−1.204197882
330260	Pon2	paraoxonase 2	−1.202091372
380787	A230065H16Rik	RIKEN cDNA A230065H16 gene	−1.243053467

* Entries in this list indicate all proteins with negative fold change > 1.2 vs WT and FDR-adjusted p<0.05